# The importance of snowmelt spatio-temporal variability for isotope-based hydrograph separation in a high-elevation catchment

Jan Schmieder[1], Florian Hanzer[1], Thomas Marke[1], Jakob Garvelmann[2], Michael Warscher[2], Harald Kunstmann[2] and Ulrich Strasser[1]

[1]Institute of Geography, University of Innsbruck, Innsbruck, 6020, Austria

[2]Institute of Meteorology and Climate Research - Atmospheric Environmental Research, Karlsruhe Institute of Technology, Garmisch-Partenkirchen, 82467, Germany

*Correspondence to*: Jan Schmieder (Jan.Schmieder@uibk.ac.at)

**Abstract.** Seasonal snow cover is an important temporary water storage in high-elevation regions. Especially in remote areas, the available data is often insufficient to explicitly quantify snowmelt contributions to streamflow. The limited knowledge about the spatio-temporal variability of the snowmelt isotopic composition, as well as pronounced spatial variation in snowmelt rates lead to high uncertainties in applying the isotope-based hydrograph separation method. The stable isotopic signatures of snowmelt water samples collected during two spring 2014 snowmelt events at a north- and a south-facing slope were volume-weighted with snowmelt rates derived from a distributed physics-based snow model in order to transfer the measured plot-scale isotopic composition of snowmelt to the catchment scale. The observed $\delta^{18}O$ values and modelled snowmelt rates showed distinct inter- and intra-event variations, as well as marked differences between north- and south-facing slopes. Accounting for these differences, two-component isotopic hydrograph separation revealed snowmelt contributions to streamflow of 35±3 % and 75±14 % for the early and peak melt season, respectively. These values differed from those determined by formerly used weighting methods (e.g. using observed plot-scale melt rates) or considering either the north- or south-facing slope by up to 5 and 15 %, respectively.

## 1 Introduction

In many headwater catchments, seasonal water availability is strongly dependent on cryospheric processes and understanding these processes becomes even more relevant in a changing climate (APCC, 2014; IPPC, 2013; Weingartner and Aschwanden, 1992).The seasonal snow cover is an important temporary water storage in alpine regions. The timing and amount of water released from this storage is important to know for water resources management, especially in downstream regions where the water is needed (drinking water, snow making, hydropower, irrigation water) or where it represents a potential risk (flood, drought). Environmental tracers are a common tool to investigate the hydrological processes, but scientific studies are still rare for high-elevation regions because of the restricted access and high risk for field measurements in these challenging conditions.

Two-component isotopic hydrograph separation (IHS) is a technique to separate streamflow into different time source components (event water, pre-event water) (Sklash et al., 1976). The event component depicts water that enters the catchment during an event (e.g. snowmelt) and is characterized by a distinct isotopic signature, whereas pre-event water is stored in the catchment prior to the onset of the event (i.e. groundwater and soil water which form baseflow) and is characterized by a different isotopic signature (Sklash and Farvolden, 1979; Sklash et al., 1976). The technique dates back to the late 1960s (Pinder and Jones, 1969) and was initially used for

separating storm hydrographs in humid catchments. The first snowmelt-based studies were conducted in the 1970s by Dincer et al. (1970) and Martinec et al. (1974). These studies showed a large pre-event water fraction (>50 %) of streamflow that changed the understanding of the processes in catchment hydrology fundamentally (Klaus and McDonnell, 2013; Sklash and Farvolden, 1979) and forced a paradigm shift, especially for humid temperate catchments. However, other snowmelt-based studies (Huth et al., 2004; Liu et al., 2004; Williams et al., 2009) reveal a large contribution of event water (>70 %), i.e. in permafrost or high-elevation catchments, depending on the system state (e.g. frost layer thickness and snow depth), catchment characteristics and runoff generation mechanisms.

Klaus and McDonnell (2013) highlighted the need to quantify and account for the spatial variability of the isotope signal of event water, which is still a vast uncertainty in snowmelt-based IHS. In the literature inconclusive results prevail with respect to the variation of the isotopic signal of snowmelt. Spatial variability of snowmelt isotopic composition was statistically significant related to elevation (Beaulieu et al., 2012) in a catchment in British Columbia, Canada with 500 m relief. Moore (1989) and Laudon et al. (2007) found no statistical significant variation in their snowmelt $\delta^{18}O$ data, due to the low gradient and small elevation range (approximately 30 m and 290 m) in their catchments, which favours an isotopically more homogenous snow cover. The effect of the aspect of the hillslopes on isotopic variability and IHS results in topographically complex terrain has also been rarely investigated. Dahlke and Lyon (2013) and Dietermann and Weiler (2013) surveyed the snowpack isotopic composition and showed a notable spatial variability in their data, particularly between north- and south-facing slopes. They conclude that the spatial variability of snowmelt could be high and that the timing of meltwater varies with the morphology of the catchment. Dietermann and Weiler (2013) also concluded that an elevation effect (decrease of snowpack isotopic signature with elevation), if observed, is disturbed by fractionation due to melt/refreeze processes during the ablation period. These effects most likely superimpose the altitudinal gradient. Aspect and slope are therefore important factors that affect the isotopic evolution of the snow cover and its melt (Cooper, 2006). In contrast, there have been various studies that have investigated the temporal variability of the snowmelt isotopic signal, e.g. by the use of snow lysimeters (Hooper and Shoemaker, 1986; Laudon et al., 2002; Liu et al., 2004; Maulé and Stein, 1990; Moore, 1989; Williams et al., 2009). During the ablation season the isotopic evolution of the snowpack progresses due to percolating rain water and fractionation caused by melting, refreezing and sublimation (Dietermann and Weiler, 2013; Lee et al., 2010; Unnikrishna et al., 2002; Zhou et al., 2008), which leads to a homogenization of the isotopic profile of the snowpack (Árnason et al., 1973; Dinçer et al., 1970; Stichler, 1987) and an increase in heavy isotopes of meltwater throughout the freshet period (Laudon et al., 2007; Taylor et al., 2001; Taylor et al., 2002; Unnikrishna et al., 2002). Therefore, the characterization and the use of the evolving isotopic signal of snowmelt water instead of single snow cores is crucial for applying IHS (Taylor et al., 2001; 2002).

There have been various approaches to cope with the temporal variability of the input signal. If one uses more than one $\delta^{18}O$ snowmelt value for applying the IHS method, it is important to weight the values with appropriate melt rates, e.g. measured from the outflow of a snow lysimeter. Common weighting methods are the volume-weighted average approach (VWA), as used by Mast et al. (1995), and the current meltwater approach (CMW), applied by Hooper and Shoemaker (1986). Laudon et al. (2002) developed the runoff-corrected event water approach (runCE), which accounts for both, the temporal isotopic evolution and temporary storage of meltwater in the catchment and overcomes the shortcoming of the exclusion of residence times by VWA and CMW. This

1 method was also deployed in several other snowmelt-based IHS (Beaulieu et al., 2012; Carey and Quinton,
2 2004; Laudon et al., 2004; Laudon et al., 2007).

3 Tracers have successfully been used in modelling studies to provide empirical insights into runoff generation
4 processes and catchment functioning (Birkel and Soulsby, 2015; Birkel et al., 2011; Capell et al., 2012;
5 Uhlenbrook and Leibundgut, 2002), but the combined use of distributed modelling and isotope tracers in snow-
6 dominated environments is rare. Ahluwalia et al. (2013) used an isotope and a modelling approach to derive
7 snowmelt contributions to streamflow and determined differences between the two techniques of 2 %.
8 Distributed modelling can provide areal melt rates that can be used for weighting the measured isotopic
9 composition of meltwater. Pomeroy et al. (2003) described the differences of insolation between north- and
10 south-facing slopes in complex terrain that lead to spatial varying melt rates of the snowpack throughout the
11 freshet period. The use of the areal snowmelt data from models will likely reduce the uncertainty that arises from
12 the representativeness of measured melt rates at the plot-scale.

13 The overall goal of our study was to quantify the contribution of snowmelt to streamflow and hence to improve
14 the knowledge of hydroclimatological processes in high-elevation catchments. This study aims to test a
15 technique to enhance the reliability of isotope-based hydrograph separation, and thus the estimation of snowmelt
16 contributions to streamflow by considering the distinct spatio-temporal variability of snowmelt and its isotopic
17 signature in a high-elevation study region. This study has the following three objectives: 1) the estimation of the
18 spatio-temporal variability of snowmelt and its isotopic composition, 2) the quantification of the impact of the
19 spatial variability in snowmelt rates and its isotopic composition on isotope-based hydrograph separation (IHS)
20 and 3) to assess the combined use of a physically-based snowmelt model and traditional IHS. Distributed melt
21 rates provided by a surface energy balance model were used to weight the measured isotopic composition of
22 snowmelt in order to characterize the event water isotopic composition. Traditional weighting methods (e.g.
23 using plot-scale observed melt rates) were compared with the model approach. This study provides an integrated
24 approach to understand the streamflow components based on experimental field work (data collection) and
25 modelling, as requested in previous studies (e.g. Seibert and McDonnell, 2002).

26 **2 Study area**

27 The 98 km$^2$ high-elevation catchment of the stream Rofenache is located in the Central Eastern Alps (Oetztal
28 Alps, Austria), close to the main Alpine ridge. The study area has a dry inner-alpine climate. Mean annual
29 precipitation is 800 mm yr$^{-1}$, of which 44 % falls as snow. The mean annual temperature at the gauging station in
30 Vent (1890 m.a.s.l., reference period: 1982-2003) is 2°C. Seasonal snow cover typically lasts from October to
31 the end of June at the highest regions of the valley. The basin ranges in elevation from approximately 1900
32 m.a.s.l. to 3770 m.a.s.l.. Average slope is 25° and average elevation is 2930 m.a.s.l. (calculated from a 50 m
33 digital elevation model). A narrow riparian zone (<100 m width) is located in the valley floor. The
34 predominantly south- (SE) and north-facing (NNW) slopes form the main valley (cf. Fig. 1a), which trends
35 roughly from southwest to northeast (cf. Fig. 1b).

36 The bedrock consists of mainly paragneiss and mica schist and is overlain by a mantle of glacial deposits and
37 thin soils (< 1 m). The bedrock outcrops and unconsolidated bare rocks cover the largest part (42 %) of the
38 catchment (CLC, 2006). Glaciers cover approximately a third of the Rofenache catchment (35 %), while pastures
39 and coniferous forests are located in the lowest parts of the catchment and cover less than 0.5 % (CLC, 2006).

1 Sparsely vegetated areas and natural grassland cover 15 and 7.5 %, respectively (CLC, 2006). Besides seasonally

2 frozen ground at slopes of various expositions, permafrost is likely to occur at an altitude over 2600 m.a.sl. at the

3 north-facing slopes (Haeberli, 1975). The annual hydrograph reveals a highly seasonal flow regime. The mean

4 annual discharge is 4.5 $m^3 s^{-1}$ (reference period: 1971-2009) and is dominated by snow and glacier melt during

5 the ablation season, which typically lasts from May to September. The onset of the early snowmelt season in the

6 lower part of the basin is typically in April.


## 3 Methods

### 3.1 Field sampling, measurements and laboratory analysis

9 The field work was conducted during the 2014 snowmelt season between the beginning of April and the end of

10 June. Two short-term melt events (3 days) were investigated to illustrate the difference between early spring

11 season melt and peak melt. The events were defined as warm and precipitation-free spells, with clear sky and dry

12 antecedent conditions (i.e. no precipitation was observed 48 h prior to the event). Low discharge and air

13 temperatures with a small diurnal variation and low melt rates, as well as a snow-covered area (SCA) of about

14 90 % in the basin (Fig. 2a) characterize the conditions of the early melt event at the end of April (cf. Fig. 3b). In

15 contrast, the peak melt period at the end of June is characterized by high discharge and melt rates, a flashy

16 hydrograph, high air temperatures with remarkable diurnal variations (Fig. 3c) and a strongly retreated snowline

17 (SCA: 66 %; cf. Fig. 2c). Discharge data are available at an hourly resolution for the gauging station in Vent and

18 meteorological data are obtained by 20 automatic weather stations (hourly resolution) located in and around the

19 basin (Fig. 1).

20 The stream water sampling for stable isotope analysis consisted of pre-freshet baseflow samples at the beginning

21 of March, sub-daily samples (temporal resolution ranges between 1 and 4 hours) during the two studied events

22 and a post-event sample in July as indicated in Fig. 3a (grey-shaded area). Samples of snowmelt, snowpack and

23 surface overland flow (if observed) were collected at the south- (S1, S2) and north-facing slope (N1, N2), as well

24 as on a wind-exposed ridge shown in Fig. 1b using a snowmelt collector. At each test site a snow pit was dug to

25 install a 0.1 $m^2$ polyethylene snowmelt collector at the ground-snowpack interface. The snowmelt collector

26 consists of a pipe that drains the percolating meltwater into a fixed plastic bag. Tests yield a preclusion of

27 evaporation for this sampling method. Composite daily snowmelt water samples (bulk sample) were collected in

28 these bags and transferred to polyethylene bottles in the field before the onset of the diurnal melt cycle.

29 Furthermore, sub-daily grab melt samples were collected at S1 (on 23 April) and at N2 (on 07 June) to define the

30 diurnal variability of the respective melt event. Unfortunately further sub-daily snowmelt sampling was not

31 feasible. The pit face was covered with white styrofoam to protect it from direct sunlight. Stream, surface

32 overland flow and grab snowmelt water samples were collected in 20 mL polyethylene bottles. Snow samples

33 from snow pit layers were filled in airtight plastic bags and melted below room temperature before transferring

34 them in bottles. Overall, 144 samples were taken during the study period. Snow water equivalent (SWE), snow

35 height (HS), snow density (SD), and various snowpack observations (wetness and hand hardness index) were

36 observed before the onset of the diurnal melt cycle at the study plots (Fig. 1). Mean SWE was determined by

37 averaging five snow tube measurements within an area of 20 $m^2$ at each site. Daily melt rates were calculated by

38 subtracting succeeding SWE values. Sublimation was neglected, as it contributes only to a small percentage (~10

39 %) to the seasonal water balance in high altitude catchments in the Alps (Strasser et al., 2008).

All samples were treated by the guidelines as proposed by Clark and Fritz (1997) and were stored dark and cold until analysis. The isotopic composition of the samples ($\delta^{18}O$, $\delta D$) was measured with cavity ring-down spectroscopy (Picarro L1102-i). Results are expressed in the delta notation as parts per thousand relative to the Vienna Standard Mean Ocean Water (VSMOW2).The mean laboratory precision (replication of 8 measurements) for all measured samples was 0.06 ‰ for $\delta^{18}O$. Due to the covariance of $\delta^2H$ ($\delta D$) and $\delta^{18}O$ (Fig. 5), all analyses were done with oxygen-18 values.

**3.2 Model description**

For the simulation of the daily melt rates, the non-calibrated, distributed, and physically-based hydroclimatological model AMUNDSEN (Strasser, 2008) was applied. Model features include interpolation of meteorological fields from point measurements (Marke, 2008; Strasser, 2008); simulation of short- and longwave radiation, including topographic and cloud effects (Corripio, 2003; Greuell et al., 1997); parameterization of snow albedo depending on snow age and temperature (Rohrer, 1992); modelling of forest snow and meteorological processes (Liston and Elder, 2006; Strasser et al., 2011); lateral redistribution of snow due to gravitational (Gruber, 2007) and wind-induced (Helfricht, 2014; Warscher et al., 2013) processes; and determination of snowmelt using an energy balance approach (Strasser, 2008). Besides having been applied for various other Alpine sites in the past (Hanzer et al., 2014; Marke et al., 2015; Pellicciotti et al., 2005; Strasser, 2008; Strasser et al., 2008; Strasser et al., 2004), AMUNDSEN has recently been set up and extensively validated for the Oetztal Alps region (Hanzer et al., 2016). This setup was also used to run the model in this study for the period 2013–2014 using a temporal resolution of 1 hour and a spatial resolution of 50 meters. In order to determine the model performance during the study period, catchment-scale snow distribution by satellite-derived binary snow cover maps and plot-scale observed SWE data were used for the validation (cf. Section 4.2). Therefore the spatial snow distribution as simulated by AMUNDSEN was compared with a set of MODIS (500 m spatial resolution) and Landsat (30 m resolution, subsequently resampled to the 50 m model resolution) snow maps with less than 10 % cloud coverage over the study area using the methodology described in Hanzer et al. (2016). Model results were evaluated using the performance measures BIAS, accuracy (ACC) and critical success index (CSI) (Zappa, 2008). ACC represents the fraction of correctly classified pixels (either snow-covered or snow-free both in the observation and the simulation). CSI describes the number of correctly predicted snow-covered pixels divided by the number of times where snow is predicted in the model and/or observed, and BIAS corresponds to the number of snow-covered pixels in the simulation divided by the respective number in the observation. ACC and CSI values range from 0 to 1 (where 1 is a perfect match), while for BIAS values below 1 indicate underestimations of the simulated snow cover, and values above 1 indicate overestimations. At the plot-scale, observed SWE values were compared with AMUNDSEN SWE values represented by the underlying pixel at the location of the snow course. Catchment-scale melt rates are calculated by subtracting two consecutive daily SWE grids, neglecting sublimation losses, as also done to achieve observed melt rates at the plot-scale. Subsequently, the DEM was used to calculate an aspect grid and further to divide the catchment into two parts: grid cells with aspects ranging from $\geq 270\,°$ to $\leq 90\,°$ were classified as 'north-facing', while the remaining cells were attributed to the class 'south-facing'. Finally, these two grids were combined to derive melt rates for the south-facing ($melt_s$) and for the north-facing slope ($melt_n$).

## 3.3 Isotopic hydrograph separation, weighting approaches and uncertainty analysis

IHS is a steady-state tracer mass balance approach and several assumptions underlie this simple principle, which are described and reviewed in Buttle (1994) and Klaus and McDonnell (2013):

(1) The isotopic compositions of event and pre-event water are significantly different.

(2) The event water isotopic signature has no spatio-temporal variability, or variations can be accounted for.

(3) The pre-event water isotopic signature has no spatio-temporal variability, or variations can be accounted for.

(4) Contributions from the vadose zone must be negligible or soil water should be isotopically similar to groundwater.

(5) There is no or minimal discharge contribution from surface storage.

The focus of this study is on one of the assumptions: the spatio-temporal variability of event water isotopic signature is absent or can be accounted for. The fraction of event water ($f_e$) contributing to streamflow was calculated from Eq. (1).

$$f_e = \frac{(c_p - c_s)}{(c_p - c_e)} \tag{1}$$

The tracer concentration of the pre-event component ($C_p$) is the $\delta^{18}O$ composition of baseflow prior to the onset of the freshet period, constituted mainly by groundwater and potentially by soil water which was assumed to have the same isotopic signal as groundwater. Tracer concentration $C_s$ is the isotopic composition of stream water for each sampling time. The isotopic compositions of snowmelt samples were weighted differently to compose the event water tracer concentration ($C_e$) using the following five weighting approaches:

(1) volume-weighted with observed plot-scale melt rates (VWO)

(2) equally weighted, assuming an equal melt rate on north- and south-facing slopes (VWE)

(3) no weighting, only south-facing slopes considered (SOUTH)

(4) no weighting, only north-facing slopes considered (NORTH)

(5) volume-weighted with simulated catchment-scale melt rates (VWS)

Equation (2) is the VWS approach with simulated melt rates for north- and south-facing slopes as described in Section 3.2, where $M$ is the simulated melt rate (in mm d$^{-1}$), $\delta^{18}O$ is the isotopic composition of sampled snowmelt and subscripts $s$ and $n$ indicate north and south, respectively. For obtaining the value of $C_e$ a daily timestep ($t$) is used, considering daily melt rates and the isotopic composition of the daily bulk snowmelt samples.

$$C_e(t) = \frac{M_s(t)\delta^{18}O_s(t) + M_n(t)\delta^{18}O_n(t)}{M_s(t) + M_n(t)} \tag{2}$$

An uncertainty analysis (Eq. (3)) was performed according to the Gaussian standard error method proposed by Genereux (1998):

$$W_{f_e} = \left\{ \left[ \frac{c_p - c_s}{(c_p - c_e)^2} W_{C_e} \right]^2 + \left[ \frac{c_s - c_e}{(c_p - c_e)^2} W_{C_p} \right]^2 + \left[ \frac{-1}{(c_p - c_e)^2} W_{C_s} \right]^2 \right\}^{1/2}, \tag{3}$$

where $W$ is the uncertainty, $C$ is the isotopic composition, $f$ is the fraction and the subscripts $p$, $s$ and $e$ refer to the pre-event, stream and event component. This assumes negligible errors in the discharge measurements and

1  the melt rates (modelled and observed). The uncertainty of streamflow ($W_{C_s}$) is assumed to be equal to the

2  laboratory precision (0.06 ‰). For the uncertainty of the event component ($W_{C_e}$), the diurnal temporal variability

3  (standard deviation) of the snowmelt isotopic signal (from one site and one day) was multiplied by the

4  appropriate value of the two-tailed t-table (dependent on sample number) and used for the event, as proposed by

5  Genereux (1998). Different uncertainty values were applied for the early melt event ($W_{C_e}$ = 0.2 ‰) and the peak

6  melt event ($W_{C_e}$ = 0.5 ‰). An error of 0.04 ‰ was assumed for the pre-event component ($W_{C_p}$), which reflects

7  the standard deviation of two baseflow samples. A 95 % confidence level was used. Spatial variation in

8  snowmelt and its isotopic composition were not considered in this error calculation method as they represent the

9  hydrologic signal of interest.

10  **4 Results**

11  **4.1. Spatio-temporal variability of streamflow and stable isotopic signature of sampled of water sources**

12  Two major snowmelt pulses (Mid-May and beginning of June) and four less pronounced ones between mid-

13  March to early May occurred during the snowmelt season (Fig. 3a). Peak melt occurred at the beginning of June

14  with maximum daily temperatures and runoff of 15 °C and 18 mm d$^{-1}$, respectively. The following high-flows

15  were affected by rain (Fig. 3a) and glacier melt due to the strongly retreated snow line and snow-free ablation

16  area of the glaciers in July. Diurnal variations in discharge were strongly correlated with diurnal variations of air

17  temperature (Fig. 3b and c) with a time lag of 3-5 hours for the early melt event and 2-3 hours for the peak melt

18  event. An inverse relationship between streamflow $\delta^{18}O$ and discharge was found for the early melt event (Fig.

19  4a and c). Small diurnal responses of streamflow $\delta^{18}O$ were identified for both events, but were masked due to

20  missing data during the recession of the hydrograph.

21  The quality control of the isotopic data was performed by the $\delta^2H$-$\delta^{18}O$ plot (Fig. 5), which indicated no shift in

22  the linear regression line and thus no secondary fractionation effects (evaporation) during storage and transport

23  of the samples. The slope of the linear regression (slope=8.5, n=144, R²=0.93) of the measurement data slightly

24  deviates from that of the global meteoric (slope=8) and local meteoric water line (slope=8.1) based on monthly

25  data from the ANIP (Austrian Network of Isotopes in Precipitation) sampling site in Obergurgl, which is located

26  in an adjacent valley (reference period: 1991-2014). The small deviation (visible in Fig. 5) of the sampled water

27  (i.e. snowpack and snowmelt) could indicate fractionation effects induced by phase transition (i.e. melt/refreeze

28  and sublimation). The significant differences between the isotopic signatures of pre-event streamflow and

29  snowmelt water enabled the IHS.

30  Overall, the complete $\delta^{18}O$ values ranged from -21.5 to -15.0 ‰, while snowpack samples were characterized by

31  the most negative and pre-event baseflow samples by the least negative values. Snowpack samples showed a

32  wide isotopic range, while streamflow samples revealed the narrowest spread, reflecting a composite isotopic

33  signal mixing of the water components. Figure 6 shows the $\delta^{18}O$ data of the water samples grouped into different

34  categories and split into early and peak melt data. It shows the different $\delta^{18}O$ ranges and medians of the sampled

35  water sources (Fig. 6a), as well as marked spatio-temporal variations in the isotopic signal (Fig. 6b and c). It is

36  apparent that the snowpack $\delta^{18}O$ values have a larger variation compared to the snowmelt data due to

37  homogenization effects (Fig. 6a), as was also shown by Árnason et al. (1973), Dincer et al. (1970) and Stichler

38  (1987). The median of the $\delta^{18}O$ of snowmelt was higher than that of the snowpack indicating fractionation. The

39  median $\delta^{18}O$ of surface overland flow was higher than that of snowmelt (Fig. 6a) for the early and peak melt

1    period. Overall, the peak melt $\delta^{18}O$ values (Fig. 6b) were less variable and had a higher median than the early

2    melt values, because fractionation effects (due to melt/refreeze and sublimation) most likely altered the isotopic

3    composition of the snowpack over time (cf. Taylor et al., 2001, 2002). One major finding was that the north-

4    facing slope $\delta^{18}O$ values had a larger range and a lower median compared to the opposing slope (Fig. 6c).

5    Samples from the wind drift influenced site (also south-exposed) were more depleted in heavy isotopes

6    compared to the south-facing slope samples (Fig. 6c).

7    In general, the average snowmelt and snowpack isotopic composition was more depleted for the early melt

8    period (Table 1) and changed over time because fractionation likely altered the snowpack and its melt. It is

9    obvious that the isotopic evolution (gradually enrichment) on the south-facing slope took place earlier in the

10   annual melting cycle of the snow, and indicates a premature snowpack concerning the enrichment of isotopes

11   and earlier ripening compared to the north-facing slope.

12   Table 1 shows that meltwater sampling throughout the entire snowmelt period is required to account for the

13   temporal variation in the isotopic composition of the snowpack (cf. Taylor et al., 2001, 2002). In detail, the

14   snowpack and snowmelt $\delta^{18}O$ data highlighted a marked spatial inhomogeneity between north- and south-facing

15   slopes throughout the study period. The snowpack isotopic composition from both sampled slopes was

16   statistically different for the early melt, but not for the peak melt (with Kruskal-Wallis test at 0.05 significance

17   level), whereas the snowmelt $\delta^{18}O$ showed a significant difference throughout the study period (Fig. 7).

18   Sub-daily snowmelt samples (n=5) at S1 (23 April 2014) had a range of 0.1 ‰ in $\delta^{18}O$, and the bulk sample

19   (integrating the entire diurnal melt cycle) was within the scatter of those values (Fig. 8). The intra-daily

20   variability of snowmelt (n=3) at N2 (07 June 2014) was relatively higher with values ranging from -17.9 to -

21   18.1 ‰. The bulk sample (-17.9 ‰) was at the upper end of those values (Fig. 8).

22   Stream water isotopic composition was more enriched in heavy isotopes during the early melt period and

23   successively became more depleted throughout the freshet period, resulting in more negative values during peak

24   melt (Table 2). The standard deviation and range of stream water $\delta^{18}O$ during early melt was higher and could be

25   related to an increasing snowmelt contribution throughout the event and larger diurnal amplitudes of snowmelt

26   contribution compared to peak melt (Table 2).

27   **4.2 Snow model validation and snowmelt variability**

28   Figure 9 shows the values for the selected performance measures based on the available MODIS and Landsat

29   scenes during the period March–July 2014. The results indicate a reasonable model performance with a tendency

30   to slightly overestimate the snow cover during the peak melt season (BIAS >1). In general the CSI does not drop

31   below 0.7 and 80 % of the pixels are correctly classified (ACC) throughout the study period. Fig. 2 shows the

32   observed and simulated spatial snow distribution around the time of the two events. Despite a higher SCA during

33   the early melt season (Fig. 2a and b) compared to the peak melt season (Fig. 2c and d) one can see the

34   overestimation of the simulated SCA compared to the observed (MODIS/Landsat) SCA. Table 3 shows the

35   observed and simulated SWE values at the plot-scale. The model slightly underestimated SWE during peak melt,

36   but generally appears to be in quite good agreement, suggesting well simulated snowpack processes. Throughout

37   the study period the model deviates by 13 % from the observed SWE values, but the representativeness (small-

38   scale effects) of SWE values represented by the respective 50 m pixel should be considered.

39   Snowmelt (observed and simulated daily losses of SWE) showed a distinct spatial variation between the north-

40   facing and the south-facing slope for the early melt (23/24 April), but less marked variations for the peak melt

8

1 (07/08 June) period (Fig. 10). Relative day-to-day differences are more pronounced for the early melt season.

2 Both simulated and observed melt rates are higher for the peak melt event on the south-facing slope, but not for

3 the north-facing slope. Simulated melt intensity on the south-facing slope at the end of April was twice the rate

4 on the north-facing slope, while simulated melt rates were approximately the same for the opposing slopes

5 during peak melt. Simulated (catchment scale) snowmelt rates were markedly higher during the early melt (23

6 and 24 April) on the north-facing slope compared to the observed (plot scale) melt rates (Fig. 10a), but

7 differences between them were small during peak melt for both slopes (07 and 08 June; Fig. 10).

8 ### 4.3 Weighting techniques and isotope-based hydrograph separation

9 Differences between the applied snowmelt weighting techniques, induced by the high spatial variability of

10 snowmelt (Section 4.2), led to different event water isotopic compositions ($C_e$) for the IHS analyses (Table 4).

11 The event water component is depleted in $\delta^{18}$O by roughly 0.3 ‰ for the second day (24 April) of the early melt

12 event compared to the preceding day, but inter-daily variation during the peak melt is almost absent. Especially

13 during early melt (23/04 to 24/04) strong deviations between observed plot-scale melt rates and distributed

14 (areal) melt rates obtained by AMUNDSEN occurred (Fig. 11), and led to more different event water isotopic

15 compositions between the VWS and the VWO approach (Table 4).

16 The hydrograph and the results of the IHS applied with the VWS method for the early and peak melt event are

17 presented in Fig. 4 and highlighted lower flow rates and higher pre-event fractions during early melt (Fig. 4c)

18 and vice versa for the peak melt period (Fig. 4d). The total runoff volume during the peak melt period was

19 approximately six times higher than in the early melt period. The fraction of snowmelt (volume) estimated with

20 the VWS approach was 35 and 75 % with calculated uncertainties (95 % confidence level) of ±3 and ±14 % for

21 the early and peak melt event, respectively. The uncertainty calculated from Eq. (3) of the IHS applied with the

22 VWS method was higher (14 %) for the peak melt event than for the early melt event because the difference

23 between isotopic composition of pre-event water and event water was smaller than for the early melt event

24 (uncertainty: 3 %) (cf. Table 2 and 4).

25 Throughout the early melt event, the snowmelt fraction increased from 25 to 44 % (Fig. 4c; Table 5). This trend

26 mirrors the stream isotopic composition, which became more depleted (Fig. 4a). Event water contributions

27 during peak melt were generally higher but had a smaller range (70 to 78 %; Fig. 4d). Diurnal isotopic variations

28 of stream water were small for both events (Fig. 4a and b), and could not clearly be obtained due to missing data

29 at the falling limb of the hydrographs.

30 The use of the different weighting approaches led to strongly varying estimated snowmelt fractions of

31 streamflow (Fig. 12). Especially the differences between the SOUTH and the NORTH approach during both

32 investigated events (up to 24 %), and the differences between the VWS and the VWO approach (5 %) during

33 early melt (Fig. 12a) are notable. Event water contributions estimated by the different weighting methods ranged

34 from 21-28 % at the beginning of the early melt event up to 31-55 % at the end of the event (cf. Fig. 12a, Table

35 6). Minimum event water contributions during the peak melt were estimated at 60-84 % and maxima ranged

36 between 67-94 % for the different weighting methods (Table 6, Fig. 12b). Beside these intra-event variations in

37 snowmelt contribution, the volumetric variations at the event-scale were smaller and ranged between 28 to 40 %

38 and 66 to 90 %, for the early and peak melt event, respectively (Table 6).

39 Considering only spatial variation of snowmelt isotopic signatures (i.e. comparing the NORTH/SOUTH

40 approach with the VWE approach) for IHS led to differences in estimated event water fractions up to 7 and 14 %

1 for the early and peak melt period, respectively (Table 6). However, considering only spatial variation in
2 snowmelt rates (i.e. comparing the VWS/VWO approach with the VWE approach) led to differences in event
3 water fraction up to 3 and 2 % for the early and peak melt period, respectively (Table 6).

4 Surface overland flow was not considered in the IHS analyses, but if applied, it would most likely increase the
5 calculated snowmelt fraction slightly. Furthermore, snowmelt samples from the wind-exposed site were not used
6 in the IHS analyses because this site was only sampled on the south-facing slope during early melt and is not
7 representative for the catchment due to its limited coverage. However, an incorporation of this data would
8 decrease the calculated snowmelt fraction by approximately 2 %.

9 **5 Discussion**

10 **5.1 Temporal variation in streamflow during the melting season**

11 Snowmelt is a major contributor to streamflow during the spring freshet period in alpine regions and large
12 amounts of snowmelt water infiltrate into the soil and recharge groundwater (Penna et al., 2014). The
13 hydrological response of the stream followed the variations of air temperature, as already observed by
14 Braithwaite and Olesen (1989) (Fig. 3a). The observed time lags (Fig. 3b and c) between maximum daily air
15 temperature and daily peak flow are common in mountain catchments (Engel et al., 2016; Schuler, 2002). During
16 peak melt, the flashy hydrograph revealed less variation in the timing of peak discharge of 7 day data
17 (cf. Fig. 3c) compared to the early melt, as well reported by Lundquist and Cayan (2002). The increase in
18 discharge coincides with decreasing streamflow $\delta^{18}O$ during the early melt event (Fig. 4a and c) and confirms
19 earlier findings of Engel et al. (2016) who identified inverse relationships between streamflow $\delta^{18}O$ and
20 discharge during several 24-hour events in an adjacent valley on the southern side of the main Alpine ridge,
21 although their findings rely on streamflow contributions from snow and glacier melt. The lower stream water
22 isotopic composition during peak melt suggests a remarkable contribution of more depleted snowmelt to
23 streamflow and therefore confirms the results of the IHS.

24 **5.2 Spatio-temporal variability of snowmelt and its isotopic signature**

25 The rate of snowmelt varies spatially in catchments with complex topography (Carey and Quinton, 2004; Dahlke
26 and Lyon, 2013; Pomeroy et al., 2003). This was also demonstrated for the Rofen valley in this study (Fig. 10,
27 Table 3). Snowmelt results from a series of processes (e.g. energy exchange snow-atmosphere) that are spatially
28 variable - especially in complex terrain. This also becomes obvious when comparing the snowmelt rates on 23
29 April 2014 in Fig. 10a. Differences of observed and simulated snowmelt rates might result from the non-
30 representativeness of point measurements for catchment averages and refer to the scale issue of data collection.
31 The peak melt period was characterised by less spatial and day-to-day variation in observed melt rates (Fig. 10).
32 The modelled daily snowmelt during this period was similar for north- and south-facing slopes, likely because of
33 higher melt rates but also a smaller snow-covered area of the south-facing slope in contrast to the north-facing
34 slope during peak melt (Fig. 11). The model performance was good for SWE (Table 3) and snow cover extent
35 (Fig. 2 and 9). The spatial variation of snowpack isotopic composition are significant, as can be seen in the
36 differences for north- and south-facing slopes, as also shown by Carey and Quinton (2004), Dahlke and Lyon
37 (2013) and Dietermann and Weiler (2013) in their high-gradient catchments, whereas there are unclear
38 differences for the spatial variation of the snowmelt isotopic signal in the literature. It is not clear to which extent

altitude is important, as Dietermann and Weiler (2013) stated that a potential elevation effect (decrease of snowmelt $\delta^{18}$O with elevation) is likely to be disturbed by melting processes (isotopic enrichment) depending on catchment morphology (aspect, slope) during the ablation period. Beaulieu et al. (2012) detected elevation as a predictor, which explained most of the variance they observed in snowmelt $\delta^{18}$O from four distributed snow lysimeters. Moore (1989) and Laudon et al. (2007) found no significant difference of $\delta^{18}$O in their lysimeter outflows, likely due to the small elevation gradient of their catchments which favours an isotopically homogenous snowpack, whereas Unnikrishna et al. (2002) found a remarkable small-scale spatial variability. An altitudinal gradient was not considered in this study, but possible effects on IHS are discussed in Section 5.6. The difference of snowmelt (not snowpack) isotopic signature between north- and south-facing slopes was clearly shown in this study. The dataset is small, but reveals clear differences induced by varying magnitudes and timing of melt due to different intensities in solar radiation on the opposing slopes (cf. Fig. 7). Temporal variability in snowmelt isotopic composition is greater for the north-facing slope compared to the south-facing slope (Fig. 7), which was also pointed out by Carey and Quinton (2004) in their subarctic catchment. Earlier homogenization in the isotopic profile of the snowpack and earlier melt out are responsible for this phenomenon (cf. Dincer et al., 1970; Unnikrishna et al., 2002). Fractionation processes likely controlled this homogenization of the snowpack between the two investigated melt events. The isotopic homogenization of the snowpack on the south-facing slope started earlier in the melting period and caused a smaller spatial and temporal variation compared the north-facing snowpack, as also reported by Unnikrishna et al. (2002) and Dincer et al. (1970). The differences between these investigated snowpacks in the early melt season were larger than in the peak melt season. This affects the IHS results, especially because the snowmelt contributions from the south- and north-facing slope - with marked isotopic differences - were distinct. Due to melt, fractionation processes proceeded and the snowpack became more homogenous throughout the snowmelt season. However, inter-daily variations of snowpack isotopic composition, especially for the north-facing slope, were still observable during the peak melt period. The gradual isotopic enrichment of the snowpack was also observed for snowmelt, as described by many others (Feng et al., 2002; Shanley et al., 2002; Taylor et al., 2001; Taylor et al., 2002; Unnikrishna et al., 2002).

Intra-daily variations of snowmelt $\delta^{18}$O could be quantified for two sites (Fig. 8). At S1 on the south-facing slope during the early melt event, the 0.1 ‰ range in $\delta^{18}$O (n=5) was smaller than the range at N2 on the north-facing slope during the peak melt event (n=3, range=0.2 ‰). This sub-daily variability is markedly smaller than the differences between the investigated slopes (cf. Table 1), which ranged from 0.8 ‰ (peak melt) to 1.4 ‰ (early melt). Unnikrishna et al. (2002) described significant temporal variations of snowmelt $\delta^{18}$O during large snowmelt events (peak melt). However, these findings could not be confirmed within in this study, probably due to the temporally limited data and should be tested with a larger dataset. The bulk sample at S1 (23 April 2014) was isotopically closer to the sub-daily values compared to the bulk sample at N2 (07 June 2014) that was at the upper range of the appropriate sub-daily samples (Fig. 7). Therefore one could argue that for the south-facing slope there is a negligible uncertainty if one uses a single snowmelt value (at one time) for IHS instead of using a bulk sample, but this is not the case for the north-facing slope (cf. Fig. 8, site N2). Unfortunately the sample numbers are small, because more frequent and more distributed sampling (at different sites) was not feasible due to logistical issues. Hence these results should be used with caution and should be investigated in further studies. If the focus and the scale of the study is not on the sub-daily variability, the authors recommend to use bulk samples, because these integrate (automatically weighed with snowmelt rate) the diurnal variations.

**5.3 Validity of isotopic hydrograph separation**

The validity of IHS relies on several assumptions (cf. Section 3.3; Buttle, 1994; Klaus and McDonnell, 2013). The assumption that the isotopic composition of event and pre-event water differ significantly (Assumption 1) was successfully proven, because the snowmelt isotopic values were markedly lower than pre-event baseflow values (cf. Table 2 and 4, Fig. 5). Spatio-temporal variations of event water isotopic composition (Assumption 2) were accounted for by collecting daily and sub-daily samples during both events throughout the freshet period and meltwater sampling at a north- and south-facing slope, respectively. The spatially variable input of event water was considered by dividing the catchment into two parts – a north- and a south-facing slope. This study supports the findings of Dahlke and Lyon (2013) and Carey and Quinton (2004), emphasizing the highly variable snowpack/snowmelt isotopic composition due to enrichment in complex topography catchments. The temporal variability of event water isotopic composition was considered by using bulk daily samples, which integrate snowmelt from the entire diurnal melting cycle, but smooth out a sub-daily signal. Because the focus of this study was more on the inter-event than the intra-daily scale, this approach seemed reliable. The spatio-temporal variability of the isotopic composition of pre-event water (Assumption 3) is a major limitation and could not be clearly identified due to a lack of data and was therefore assumed to be constant. Small differences between the pre-event samples (-15.00 ‰ and -15.05 ‰ for $\delta^{18}O$) and post-event stream water isotopic composition support this assumption (Table 2). The assumption of soil water having the same isotopic composition as groundwater in time and space (Assumption 4) is quite critical. Some studies reveal no significant differences (e.g. Laudon et al., 2007), whereas others do (e.g Sklash and Farvolden 1979). Isotopic differences between groundwater and soil water were not considered due to a lack of data. Furthermore, it is not known to which degree the vadose zone contributes to baseflow in the study area. Winter baseflow used in the analyses is assumed to integrate mainly groundwater and partly soil water. Soil water could be hypothesized to have a negligible contribution to baseflow during winter due to the recession of the soil storage in autumn and frozen soils in winter. The assumption that no or minimal surface storage occurs (Assumption 5) is plausible because water bodies like lakes or wetlands do not exist in the study catchment and due to the steep topography detention storage is likely limited. The transit time of snowmelt was assumed to be less than 24 h. This short travel time is characteristic for headwater catchments (Lundquist et al., 2005) with high in-channel flow velocities, steep hillslopes, a high drainage density with snow-fed tributaries, thin soils, most snowmelt originating from the edge of the snow-line (small average travel distances), partly frozen soil, and observed surface overland flow. The state-of-the-art method (runCE) to include residence times of snowmelt in the event water reservoir proposed by Laudon et al. (2002) was applied in several IHS studies (Beaulieu et al., 2012; Carey and Quinton, 2004; Petrone et al., 2007), but was not feasible due to the short-term character and temporally limited data of the experimental design.

**5.4 Hydrograph separation results and inferred runoff generation processes**

High contributions from snowmelt to streamflow are common in high-elevation catchments. Daily contributions between 35 and 75 % in the Rofen valley are comparable to the results of studies conducted in other mountainous regions, mostly outside the European Alps. Beaulieu et al. (2012) estimated snowmelt contributions ranging from 7 to 66 % at the seasonal scale for their 2.4 km² catchment and reported contributions of 34 and

62 %, for the early melt and peak melt, respectively. The hydrograph is dominated by pre-event water during early melt in April (Fig. 4c), which is in accordance with the results obtained by other IHS studies (Beaulieu et al., 2012; Laudon et al., 2004; Laudon et al., 2007; Moore, 1989). The snowmelt contribution increased as the freshet period progressed and peaked with high contributions at the beginning of June. Beaulieu et al. (2012) and Sueker et al. (2000) reported comparable results for their physically similar catchments during peak melt with 62 and up to 76 % event water contributions to streamflow, respectively. At the event-scale comparable studies are rare. Engel et al. (2016) report a maximum daily snowmelt contribution estimated with a three-component hydrograph separation of 33 % for an 11 km² catchment southwest of the Rofen valley with similar physiographic characteristics, but on the southern side of the main Alpine ridge. It should be mentioned that in their study, runoff was fed by three components (snowmelt, glacier melt and groundwater) and lower snowmelt contributions were prevalent because most of the catchment area (69 %) was snow-free.

Initial snowmelt events flush the pre-event water reservoir as snowmelt infiltrates into the soil and causes the pre-event water to exfiltrate and contribute to the streamflow. As the soil and groundwater reservoir becomes gradually filled with new water (snowmelt), the event water fraction in the stream increases. The system is also wetter during peak melt. The dominance of event water in the hydrograph is interpreted as an outflow of pre-event water stored in the subsurface and the gradual replenishment of the soil and groundwater reservoirs by event water. The higher water table – compared to the early melt period – could cause a transmissivity feedback mechanism (Bishop, 1991). This is a common mechanism in catchments with glacial till (Bishop et al., 2011) characterised by higher transmissivities and hence increased lateral flow velocities towards to the surface. Runoff generation is spatially very variable in the study area. There are areas (meadow patches between rock fields) where saturation excess overland flow is dominant (observed mainly at plots S1, S2 and Wind) and areas (with larger rocks and debris) where rapid shallow subsurface flow can be assumed (plot N2). Catchment morphology controls various hydrologic processes and hence the shape of the hydrograph. Upslope residence times of snowmelt are usually smaller due to thinner soils (observed during the field work), steeper slopes (Sueker et al., 2000) and higher contributing areas of glaciers with impermeable ice (Behrens, 1978) and would be indicators for the more flashy hydrograph during the peak melt season.

**5.5 Impact of spatial varying snowmelt and its isotopic composition on IHS (Assessment of weighting approaches)**

Klaus and McDonnell (2013) stress in their review paper the need for investigating the effects of the spatially varying snowmelt and its isotopic composition on IHS. This study quantified the impact of the spatially varying isotopic composition of snowmelt between north- and south facing slopes on IHS results for the first time. The difference in volumetric snowmelt contribution to streamflow at the event-scale determined using the five different weighting methods for IHS is maximal 24 % (NORTH approach vs. SOUTH approach). The data show that the variations between the weighting approaches (VWS, VWO and VWE) are higher throughout the early melt season (Table 6), because small-scale variability of snowmelt and its isotopic composition are more pronounced in the early melt season. Thus the influence of spatial variability of snowmelt and its isotopic composition on the event water fraction calculated with IHS is larger during this time. Melt rates strongly differ between the south- and the north-facing slope (Fig. 11), which was deceptively gathered by manually measured SWE, likely due to micro-topographic effects. As the contributions from both slopes are used in Eq. (3), they strongly influence the applied weighting technique. The weighting method SOUTH (or NORTH) represents the

1   hypothetical and most extreme scenario in which only one sampling site is used for the IHS analysis. Because
2   snowmelt is more depleted in $\delta^{18}$O and closer to pre-event water isotopic composition on the south-facing slope
3   during peak melt, this scenario has the greatest effect on IHS and leads to the strongest deviation in estimated
4   snowmelt fractions (up to 15 % overestimation compared to the VWS approach). These scenarios
5   (NORTH/SOUTH) are theoretical and it is obvious that it is not recommended to conduct a IHS analysis by
6   using only samples from either north- or south-facing slopes in catchments with complex terrain. Similar to the
7   VWE method, snowmelt isotopic data was not volume-weighted in other studies (e.g. Engel et al., 2016) where
8   snowmelt data was not available. This has a more distinct effect on IHS during the early melt season because of
9   the higher spatio-temporal variability in snowmelt (and its isotopic composition) compared to the peak melt
10  season and led to a deviation in the snowmelt fraction in streamflow of 2 % and 3 % compared to the VWS and
11  VWO approach, respectively. These differences are small, because the differing snowmelt and isotopic values
12  offset each other in this particular case (Table 6). Nevertheless the results of VWS are more correct for the right
13  reason, because single observed plot-scale melt rates do not represent distributed snowmelt contribution at the
14  catchment-scale. Therefore one can hypothesize that distributed simulated melt rates enhance the reliability and
15  feasibility of IHS, whereas plot-scale weighting introduces a very large error caused by the difficulty in finding
16  locations that represent the melt rate in complex terrain. The IHS results were more sensitive to the spatial
17  variability of snowmelt $\delta^{18}$O, than spatial variations of snowmelt rates (Table 6). This is even more pronounced
18  for the peak melt period, because snowmelt rates were similar for the north- and south-facing slope, probably
19  due to a ripe snow cover throughout the catchment.

20  **5.6 Limitations of the study**

21  Collecting water samples in high-elevation terrain is challenging due to limited access and high risk (e.g.
22  avalanches), limiting high-frequency sampling. Hence some limitations are inherent in this study. Potential
23  elevation effects on snowmelt isotopic composition were not tested. The opposing sampling sites (S1-N1 and S2-
24  N2) were at the same elevation (Fig. 1). It was assumed that the differences of north- and south-facing slopes
25  were much greater than a possible altitudinal gradient in snowmelt isotopic composition. This hypothesis was
26  not tested, but based on the results of other studies (Dietermann and Weiler, 2013). However, accounting for a
27  potential altitudinal gradient (decrease of snowmelt $\delta^{18}$O with elevation) would lead to more depleted isotopic
28  signatures of event water and hence to lower event water fractions. Another disadvantage is that no snow survey
29  was conducted prior to the onset of snowmelt (peak accumulation) to estimate spatial variability in bulk snow
30  $\delta^{18}$O. Because snowmelt is used for applying IHS, it is not clear to which degree the spatial variability of the
31  snowpack isotopic composition is important. Two-component isotopic hydrograph separation was successfully
32  applied using the end-members snowmelt and baseflow, but potential contributions of glacier melt were
33  neglected (here defined as ice/firn melt). Because glaciers in the catchment were still covered by snow during the
34  peak melt season, a significant contribution from ice/firn melt was assumed to be unlikely. Nevertheless
35  negligible amounts of basal (ice) meltwater could originate from temperate glaciers. No samples could be
36  collected during the recession of the hydrograph (at night). Even though the spatial variability of the event water
37  signal was the focus of the study, only temporal variability was considered in the Genereux-based uncertainty
38  analyses. Although the temporal variability of winter baseflow isotopic composition seems to be insignificant,
39  the sample number (n=2) could be too small to characterize the pre-event component and should be clearly
40  investigated in future work. Penna et al. (2016) used two approaches to determine the isotopic composition of

pre-event water and described differences in the estimated event water contributions during snowmelt events. They advise to take pre-event samples prior to the onset of the melt season, because using pre-event samples taken prior to the onset of the diurnal melt cycle could be affected by snowmelt water from the previous melt pulses and therefore could lead to underestimated snowmelt fractions and high uncertainties. Furthermore, model results and observed discharges were assumed to be free of error in the analyses. As pointed out, instrumentation and accessibility are major problems for high-elevation studies and their sampling strategies. For this study it turned out that composite snowmelt samples were easier to collect, representing the day-integrated melt signal. A denser network of melt collectors would be desirable, as well as a snow lysimeter to gain high-frequency data automatically. Representative samples of the elevation zones and different vegetation belts could be important too, especially in partly forested catchments with a distinct relief (cf. Unnikrishna et al., 2002).

**6 Conclusions**

This study provides new insights into the variability of the isotopic composition in snowmelt and highlights its impact on IHS results in a high-elevation environment. The spatial variability in snowmelt isotopic signature was considered by experimental investigations on south- and north-facing slopes to define the isotopic composition of the snowmelt end-member with greater accuracy. This study clearly shows that distributed snowmelt rates simulated by a model, fed with meteorological data from local automatic weather stations, affect the weighting of the event water isotopic signal, and hence the estimation of the snowmelt fraction in the stream by IHS. The study provides a variety of relevant findings that are important for hydrologic research in high-alpine environments. There was a distinct spatial variability in snowmelt between north- and south-facing slopes shown for this complex terrain, especially during the early melt season. The isotopic composition of snowmelt water was significantly different between north-facing and south-facing slopes, which resulted in a pronounced effect on the estimated snowmelt contributions to streamflow with IHS. The differences in the estimated snowmelt fraction due to the weighting methods used for IHS were as large as 24 %. This study also shows that it is hardly possible to characterize the event water signature of larger slopes based on plot-scale snowmelt measurements. Applying a distributed model reduced the uncertainty of the spatial snowmelt variability inherent in point-scale observations. Hence, applying the VWS method provided more reasonable results than the VWO method. This study highlighted that sampling north- and south-facing slopes is of major importance in conducting snowmelt-based IHS in mountainous catchments with complex topography in which a non-uniform input of snowmelt can be expected, and that the selection of sampling sites has a major effect on IHS results. Sampling at least north-facing and south-facing slopes in complex terrain and using distributed melt rates to weight the snowmelt isotopic composition of the differing exposures is therefore highly recommended for applying snowmelt-based IHS.

1    **References**

2    Ahluwalia, R. S., Rai, S. P., Jain, S. K., Kumar, B., and Dobhal, D. P.: Assessment of snowmelt runoff

3    modelling and isotope analysis: a case study from the western Himalaya, India, Annals of Glaciology, 54, 299-

4    304, doi:10.3189/2013AoG62A133, 2013.

5    APCC: Austrian Assessment Report (AAR14). Summary for Policymakers (SPM), Austrian Panel on Climate

6    Change, Vienna, Austria, 2014.

7    Árnason, B., Buason, T., Martinec, J., and Theodorson, P.: Movement of water through snowpack traced by

8    deuterium and tritium. In: The role of snow and ice in hydrology. Proc. Banff Symp., UNESCO-WMO-IAHS

9    (Ed.), IAHS Publ. No., 107, 1973.

10   Beaulieu, M., Schreier, H., and Jost, G.: A shifting hydrological regime: a field investigation of snowmelt runoff

11   processes and their connection to summer base flow, Sunshine Coast, British Columbia, Hydrological Processes,

12   26, 2672-2682, doi:10.1002/hyp.9404, 2012.

13   Behrens, H., Moser, H. , Oerter, H. , Rauert, W. , Stichler, W. and Ambach, W.: Models for the runoff from a

14   glaciated catchment area using measurements of environmental isotope contents, 1978, 829-846.

15   Birkel, C. and Soulsby, C.: Advancing tracer-aided rainfall-runoff modelling: a review of progress, problems and

16   unrealised potential, Hydrological Processes, 29, 5227-5240, doi:10.1002/hyp.10594, 2015.

17   Birkel, C., Tetzlaff, D., Dunn, S. M., and Soulsby, C.: Using time domain and geographic source tracers to

18   conceptualize streamflow generation processes in lumped rainfall-runoff models, Water Resources Research, 47,

19   W02515, doi:10.1029/2010WR009547, 2011.

20   Bishop, K.: Episodic increase in stream acidity, catchment flow pathways and hydrograph separation, 1991.

21   Bishop, K., Seibert, J., Nyberg, L., and Rodhe, A.: Water storage in a till catchment. II: Implications of

22   transmissivity feedback for flow paths and turnover times, Hydrological Processes, 25, 3950-3959,

23   doi:10.1002/hyp.8355, 2011.

24   Braithwaite, R. J. and Olesen, O. B.: Calculation of glacier ablation from air temperature, West Greenland. In:

25   Glacier Fluctuations and Climatic Change, Glaciology and Quaternary Geology, Oerlemans, J. (Ed.), Kluwer

26   Academic Publisher, Dordrecht, 1989.

27   Buttle, J. M.: Isotope hydrograph separations and rapid delivery of pre-event water from drainage basins,

28   Progress in Physical Geography, 18, 16-41, doi:10.1177/030913339401800102, 1994.

29   Capell, R., Tetzlaff, D., and Soulsby, C.: Can time domain and source area tracers reduce uncertainty in rainfall-

30   runoff models in larger heterogeneous catchments?, Water Resources Research, 48, W09544,

31   doi:10.1029/2011WR011543, 2012.

32   Carey, S. K. and Quinton, W. L.: Evaluating snowmelt rnoff generation in a discontinuous permafrost catchment

33   using stable isotope, hydrochemical and hydrometric data, Nordic Hydrology, 35, 309-324, 2004.

34   Clark, I. D. and Fritz, P.: Environmental Isotopes in Hydrogeology, Lewis Publishers, Ney York, 1997.

35   CLC: Corine Land Cover 2006 raster data. European Environment Agency. The European Topic Centre on Land

36   Use and Spatial Information. 2006.

37   Cooper, L. W.: Isotopic fractionation in snow cover. In: Isotope tracers in catchment hydrology, Kendall, C. and

38   McDonnell, J. J. (Eds.), Elsevier Science, Amsterdam, Netherlands, 2006.

39   Corripio, J. G.: Vectorial algebra algorithms for calculating terrain parameters from DEMs and the position of

40   the sun for solar radiation modelling in mountainous terrain, International Journal of Geographical Information

41   Science, 17, 1-23, 2003.

1  Dahlke, H. E. and Lyon, S. W.: Early melt season snowpack isotopic evolution in the Tarfala valley, northern

2  Sweden, Annals of Glaciology, 54, 149-156, doi:10.3189/2013AoG62A232, 2013.

3  Dietermann, N. and Weiler, M.: Spatial distribution of stable water isotopes in alpine snow cover, Hydrology

4  and Earth System Sciences, 17, 2657-2668, doi:10.5194/hess-17-2657-2013, 2013.

5  Dinçer, T., Payne, B. R., Florkowski, T., Martinec, J., and Tongiorgi, E.: Snowmelt runoff from measurements

6  of tritium and oxygen-18, Water Resources Research, 6, 110-124, doi:10.1029/WR006i001p00110, 1970.

7  Engel, M., Penna, D., Bertoldi, G., Dell'Agnese, A., Soulsby, C., and Comiti, F.: Identifying run-off

8  contributions during melt-induced run-off events in a glacierized alpine catchment, Hydrological Processes, 30,

9  343-364, doi:10.1002/hyp.10577, 2016.

10 Feng, X., Taylor, S., Renshaw, C. E., and Kirchner, J. W.: Isotopic evolution of snowmelt 1. A physically based

11 one-dimensional model, Water Resources Research, 38, 35-31-35-38, doi:10.1029/2001WR000814, 2002.

12 Genereux, D.: Quantifying uncertainty in tracer-based hydrograph separations, Water Resources Research, 34,

13 915-919, doi:10.1029/98WR00010, 1998.

14 Greuell, W., Knap, W. H., and Smeets, P. C.: Elevational changes in meteorological variables along a

15 midlatitude glacier during summer, Journal of Geophysical Research: Atmospheres, 102, 25941-25954,

16 doi:10.1029/97JD02083, 1997.

17 Gruber, S.: A mass-conserving fast algorithm to parameterize gravitational transport and deposition using digital

18 elevation models, Water Resources Research, 43, W06412, doi:10.1029/2006WR004868, 2007.

19 Haeberli, W.: Untersuchungen zur Verbreitung von Permafrost zwischen Flüelapass und Piz Grialetsch

20 (Graubünden), 1975.

21 Hanzer, F., Helfricht, K., Marke, T., and Strasser, U.: Multilevel spatiotemporal validation of snow/ice mass

22 balance and runoff modeling in glacierized catchments, The Cryosphere, 10, 1859-1881, doi:10.5194/tc-10-

23 1859-2016, 2016..

24 Hanzer, F., Marke, T., and Strasser, U.: Distributed, explicit modeling of technical snow production for a ski

25 area in the Schladming region (Austrian Alps), Cold Regions Science and Technology, 108, 113-124,

26 doi:http://dx.doi.org/10.1016/j.coldregions.2014.08.003, 2014.

27 Helfricht, K.: Analysis of the spatial and temporal variation of seasonal snow accumulation in Alpine catchments

28 using airborne laser scanning. Basic research for the adaptation of spatially distributed hydrological models to

29 mountain regions, PhD, University of Innsbruck, Innsbruck, 134 pp., 2014.

30 Hock, R.: Temperature index melt modelling in mountain areas, Journal of Hydrology, 282, 104-115,

31 doi:10.1016/S0022-1694(03)00257-9, 2003.

32 Hooper, R. P. and Shoemaker, C. A.: A Comparison of Chemical and Isotopic Hydrograph Separation, Water

33 Resources Research, 22, 1444-1454, doi:10.1029/WR022i010p01444, 1986.

34 Huth, A. K., Leydecker, A., Sickman, J. O., and Bales, R. C.: A two-component hydrograph separation for three

35 high-elevation catchments in the Sierra Nevada, California, Hydrological Processes, 18, 1721-1733,

36 doi:10.1002/hyp.1414, 2004.

37 IPPC: Summary for Policymakers. Climate Change 2013: The Physical Science Basis. Contribution of Working

38 Group I to the Fifth Assessment Report of the Intergovernmental Panel on Climate Change, Cambridge, United

39 Kindom and New York, NY,USA., 2013.

40 Klaus, J. and McDonnell, J. J.: Hydrograph separation using stable isotopes: Review and evaluation, Journal of

41 Hydrology, 505, 47-64, doi:10.1016/j.jhydrol.2013.09.006, 2013.

Laudon, H., Hemond, H. F., Krouse, R., and Bishop, K. H.: Oxygen 18 fractionation during snowmelt: Implications for spring flood hydrograph separation, Water Resources Research, 38, 40-41-40-10, doi:10.1029/2002WR001510, 2002.

Laudon, H., Seibert, J., Köhler, S., and Bishop, K.: Hydrological flow paths during snowmelt: Congruence between hydrometric measurements and oxygen 18 in meltwater, soil water, and runoff, Water Resources Research, 40, W03102, doi:10.1029/2003WR002455, 2004.

Laudon, H., Sjöblom, V., Buffam, I., Seibert, J., and Mörth, M.: The role of catchment scale and landscape characteristics for runoff generation of boreal streams, Journal of Hydrology, 344, 198-209, doi:10.1016/j.jhydrol.2007.07.010, 2007.

Lee, J., Feng, X., Faiia, A. M., Posmentier, E. S., Kirchner, J. W., Osterhuber, R., and Taylor, S.: Isotopic evolution of a seasonal snowcover and its melt by isotopic exchange between liquid water and ice, Chemical Geology, 270, 126-134, doi:10.1016/j.chemgeo.2009.11.011, 2010.

Liston, G. E. and Elder, K.: A Distributed Snow-Evolution Modeling System (SnowModel), Journal of Hydrometeorology, 7, 1259-1276, doi:10.1175/JHM548.1, 2006.

Liu, F., Williams, M. W., and Caine, N.: Source waters and flow paths in an alpine catchment, Colorado Front Range, United States, Water Resources Research, 40, 1-16, doi:10.1029/2004WR003076, 2004.

Lundquist, J. D. and Cayan, D. R.: Seasonal and Spatial Patterns in Diurnal Cycles in Streamflow in the Western United States, Journal of Hydrometeorology, 3, 591-603, doi:10.1175/1525-7541(2002)003<0591:SASPID>2.0.CO;2, 2002.

Lundquist, J. D., Dettinger, M. D., and Cayan, D. R.: Snow-fed streamflow timing at different basin scales: Case study of the Tuolumne River above Hetch Hetchy, Yosemite, California, Water Resources Research, 41, W07005, doi:10.1029/2004WR003933, 2005.

Marke, T.: Development and Application of a Model Interface to couple Regional Climate Models with Land Surface Models for Climate Change Risk Assessment in the Upper Danube Watershed,Dissertation der Fakultät für Geowissenschaften, Digitale Hochschulschriften der LMU München, München, 2008.

Marke, T., Strasser, U., Hanzer, F., Stötter, J., Wilcke, R. A. I., and Gobiet, A.: Scenarios of Future Snow Conditions in Styria (Austrian Alps), Journal of Hydrometeorology, 16, 261-277, doi:10.1175/JHM-D-14-0035.1, 2015.

Martinec, J., Siegenthaler, U., Oeschger, H., and Tongiorgi, E.: New insights into the run-off mechanism by environmental isotopes. In: Isotope techniques in groundwater hydrology, Symposium, P. o. a. I. (Ed.), IAEA, Vienna, Austria, 1974.

Mast, A. M., Kendall, K., Campbell, D. H., Clow, D. W., and Back, J.: Determination of hydrologic pathways in an alpine-subalpine basin using isotopic and chemical tracers, Loch Vale Watershed, Colorado, Usa. In: IAHS Publ. Ser. Proc. Rep.Int. Assoc. Hydrol. SCI., 1995.

Maulé, C. P. and Stein, J.: Hydrologic Flow Path Definition and Partitioning of Spring Meltwater, Water Resources Research, 26, 2959-2970, doi:10.1029/WR026i012p02959, 1990.

Moore, R. D.: Tracing runoff sources with deuterium and oxygen-88 during spring melt in a headwater catchment, southern Laurentians, Quebec, Journal of Hydrology, 112, 135-148, doi:http://dx.doi.org/10.1016/0022-1694(89)90185-6, 1989.

1  Pellicciotti, F., Brock, B., Strasser, U., Burlando, P., Funk, M., and Corripio, J.: An enhanced temperature-index
2  glacier melt model including the shortwave radiation balance: development and testing for Haut Glacier d'Arolla,
3  Switzerland, Journal of Glaciology, 51, 573-587, 2005.

4  Penna, D., van Meerveld, H. J., Zuecco, G., Dalla Fontana, G., and Borga, M.: Hydrological response of an
5  Alpine catchment to rainfall and snowmelt events, Journal of Hydrology, 537, 382-397,
6  doi:http://dx.doi.org/10.1016/j.jhydrol.2016.03.040, 2016.

7  Penna, D., Engel, M., Mao, L., Dell'Agnese, A., Bertoldi, G., and Comiti, F.: Tracer-based analysis of spatial and
8  temporal variations of water sources in a glacierized catchment, Hydrology and Earth System Sciences, 18,
9  5271-5288, doi:10.5194/hess-18-5271-2014, 2014.

10  Petrone, K., Buffam, I., and Laudon, H.: Hydrologic and biotic control of nitrogen export during snowmelt: A
11  combined conservative and reactive tracer approach, Water Resources Research, 43, 1-13,
12  doi:10.1029/2006WR005286, 2007.

13  Pinder, G. F. and Jones, J. F.: Determination of the ground-water component of peak discharge from the
14  chemistry of total runoff, Water Resources Research, 5, 438-445, doi:10.1029/WR005i002p00438, 1969.

15  Pomeroy, J. W., Toth, B., Granger, R. J., Hedstrom, N. R., and Essery, R. L. H.: Variation in Surface Energetics
16  during Snowmelt in a Subarctic Mountain Catchment, Journal of Hydrometeorology, 4, 702-719,
17  doi:10.1175/1525-7541(2003)004<0702:VISEDS>2.0.CO;2, 2003.

18  Rohrer, M. B.: Die Schneedecke im Schweizer Alpenraum und ihre Modellierung, ETH, Zürich, 1992.

19  Schuler, T.: Investigation of water drainage through an alpine glacier by tracer experiments and numerical
20  modeling., 2002.

21  Seibert, J. and McDonnell, J. J.: On the dialog between experimentalist and modeler in catchment hydrology:
22  Use of soft data for multicriteria model calibration, Water Resources Research, 38, 23-21-23-14,
23  doi:10.1029/2001WR000978, 2002.

24  Shanley, J. B., Kendall, C., Smith, T. E., Wolock, D. M., and McDonnell, J. J.: Controls on old and new water
25  contributions to stream flow at some nested catchments in Vermont, USA, Hydrological Processes, 16, 589-609,
26  doi:10.1002/hyp.312, 2002.

27  Sklash, M. G. and Farvolden, R. N.: The role of groundwater in storm runoff, Journal of Hydrology, 43, 45-65,
28  doi:10.1016/0022-1694(79)90164-1, 1979.

29  Sklash, M. G., Farvolden, R. N., and Fritz, P.: A conceptual model of watershed response to rainfall, developed
30  through the use of oxygen-18 as a natural tracer, Canadian Journal of Earth Sciences, 13, 271-283,
31  doi:10.1139/e76-029, 1976.

32  Stichler, W.: Snowcover and Snowmelt Processes Studied by Means of Environmental Isotopes. In: Seasonal
33  Snowcovers: Physics, Chemistry, Hydrology, Jones, H. G. and Orville-Thomas, W. J. (Eds.), D. Reidel
34  Publishing Company, Dordrecht, Holland, 1987.

35  Strasser, U.: Modelling of the mountain snow cover in the Berchtesgaden National Park, Research Rep., 2008.

36  Strasser, U., Bernhardt, M., Weber, M., Liston, G. E., and Mauser, W.: Is snow sublimation important in the
37  alpine water balance?, The Cryosphere, 2, 53-66, doi:10.5194/tc-2-53-2008, 2008.

38  Strasser, U., Corripio, J., Pellicciotti, F., Burlando, P., Brock, B., and Funk, M.: Spatial and temporal variability
39  of meteorological variables at Haut Glacier d'Arolla (Switzerland) during the ablation season 2001:
40  Measurements and simulations, Journal of Geophysical Research: Atmospheres, 109, D03103,
41  doi:10.1029/2003JD003973, 2004.

Strasser, U., Warscher, M., and Liston, G. E.: Modeling Snow–Canopy Processes on an Idealized Mountain, Journal of Hydrometeorology, 12, 663-677, doi:10.1175/2011JHM1344.1, 2011.

Sueker, J. K., Ryan, J. N., Kendall, C., and Jarrett, R. D.: Determination of hydrologic pathways during snowmelt for alpine/subalpine basins, Rocky Mountain National Park, Colorado, Water Resources Research, 36, 63-75, doi:10.1029/1999WR900296, 2000.

Taylor, S., Feng, X., Kirchner, J. W., Osterhuber, R., Klaue, B., and Renshaw, C. E.: Isotopic evolution of a seasonal snowpack and its melt, Water Resources Research, 37, 759-769, doi:10.1029/2000WR900341, 2001.

Taylor, S., Feng, X., Williams, M., and McNamara, J.: How isotopic fractionation of snowmelt affects hydrograph separation, Hydrological Processes, 16, 3683-3690, doi:10.1002/hyp.1232, 2002.

Uhlenbrook, S. and Leibundgut, C.: Process-oriented catchment modelling and multiple-response validation, Hydrological Processes, 16, 423-440, doi:10.1002/hyp.330, 2002.

Unnikrishna, P. V., McDonnell, J. J., and Kendall, C.: Isotope variations ni a Sierra Nevada snowpack and their relation to meltwater, 260, 38-57, 2002.

Warscher, M., Strasser, U., Kraller, G., Marke, T., Franz, H., and Kunstmann, H.: Performance of complex snow cover descriptions in a distributed hydrological model system: A case study for the high Alpine terrain of the Berchtesgaden Alps, Water Resources Research, 49, 2619-2637, doi:10.1002/wrcr.20219, 2013.

Weingartner, R. and Aschwanden, H.: Discharge regime - the basis for the estimation of average flows. In: Hydrological Atlas of Switzerland, 1992.

Williams, M. W., Seibold, C., and Chowanski, K.: Storage and release of solutes from a subalpine seasonal snowpack: soil and stream water response, Niwot Ridge, Colorado, Biogeochemistry, 95, 77-94, doi:10.1007/s10533-009-9288-x, 2009.

Zappa, M.: Objective quantitative spatial verification of distributed snow cover simulations—an experiment for the whole of Switzerland, Hydrological Sciences Journal, 53, 179-191, doi:10.1623/hysj.53.1.179, 2008.

Zhou, S., Nakawo, M., Hashimoto, S., and Sakai, A.: The effect of refreezing on the isotopic composition of melting snowpack, Hydrological Processes, 22, 873-882, doi:10.1002/hyp.6662, 2008.
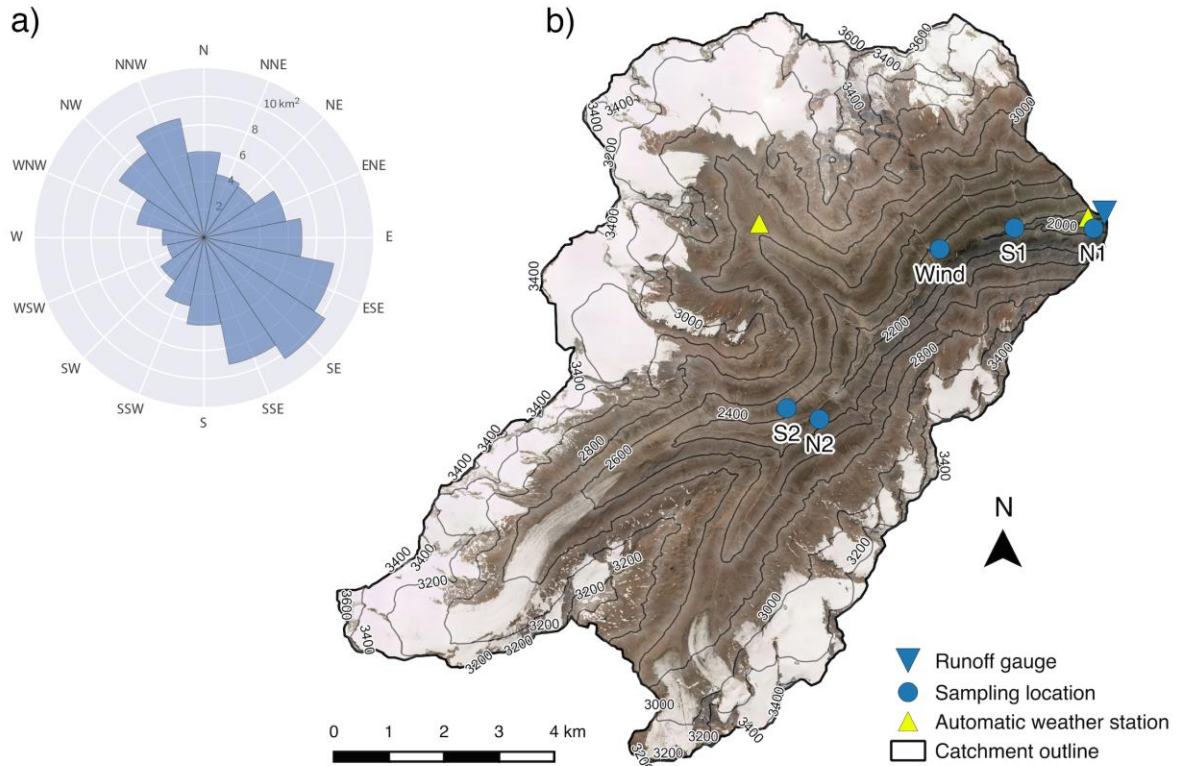
Figure 1: (a) Distribution of slope aspects in the study area; (b) Study area (Rofen valley) with underlying orthophoto, sampling and measurement locations.
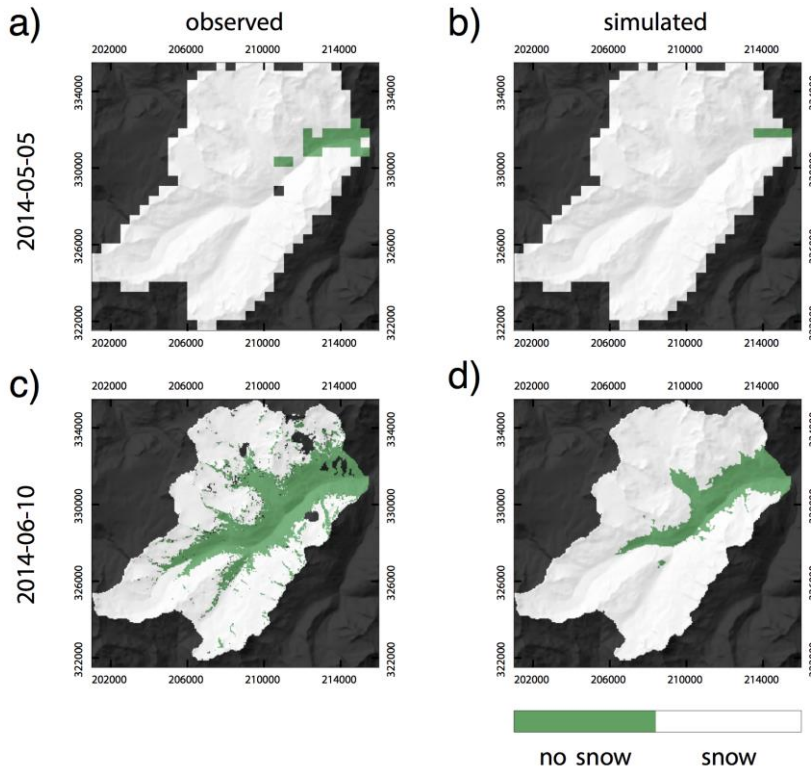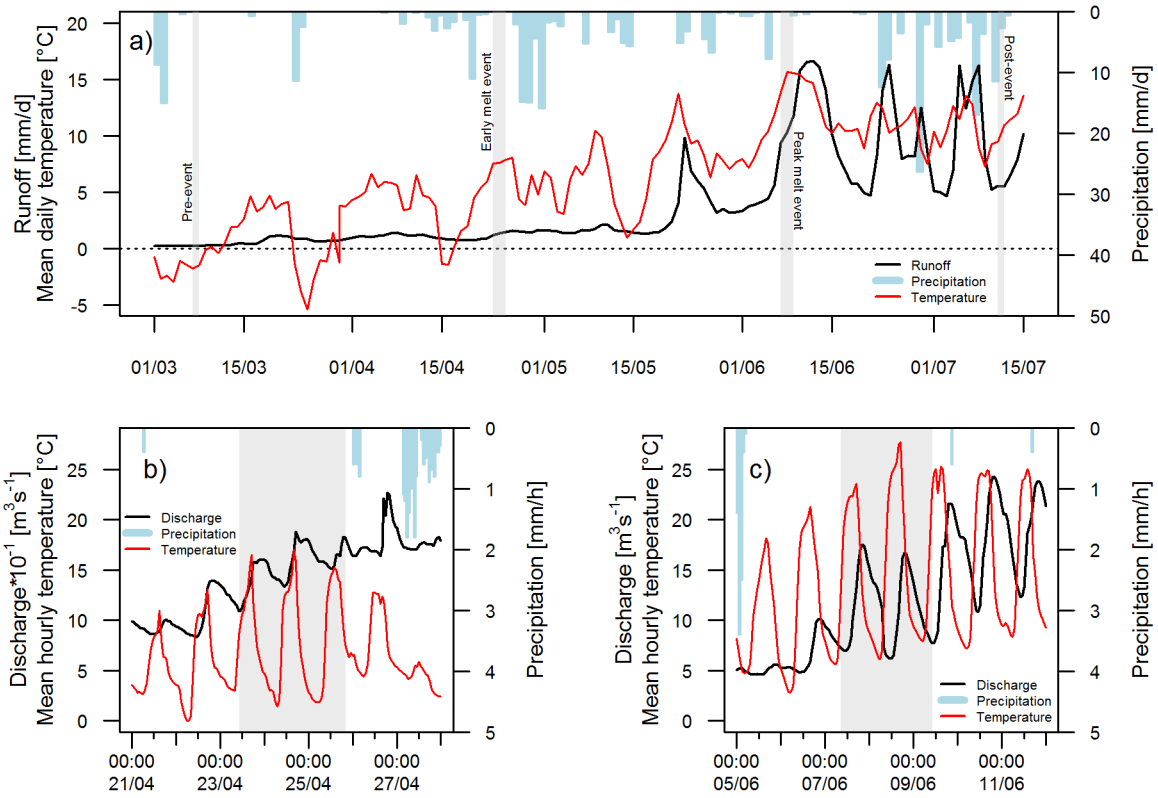


Figure 2: Comparison of observed and simulated snow distributions for (a, b) May 5 (MODIS scene) and (c, d) June 10, 2014 (Landsat scene).

1



2

3  **Figure 3: (a) Daily precipitation, air temperature, and discharge during the complete study period; Hourly hydro-**
4  **climatologic data of a 7-day period around the (b) early melt and (c) peak melt event. Data was measured at the outlet**
5  **of the catchment. Grey-shaded areas indicate the investigated events.**
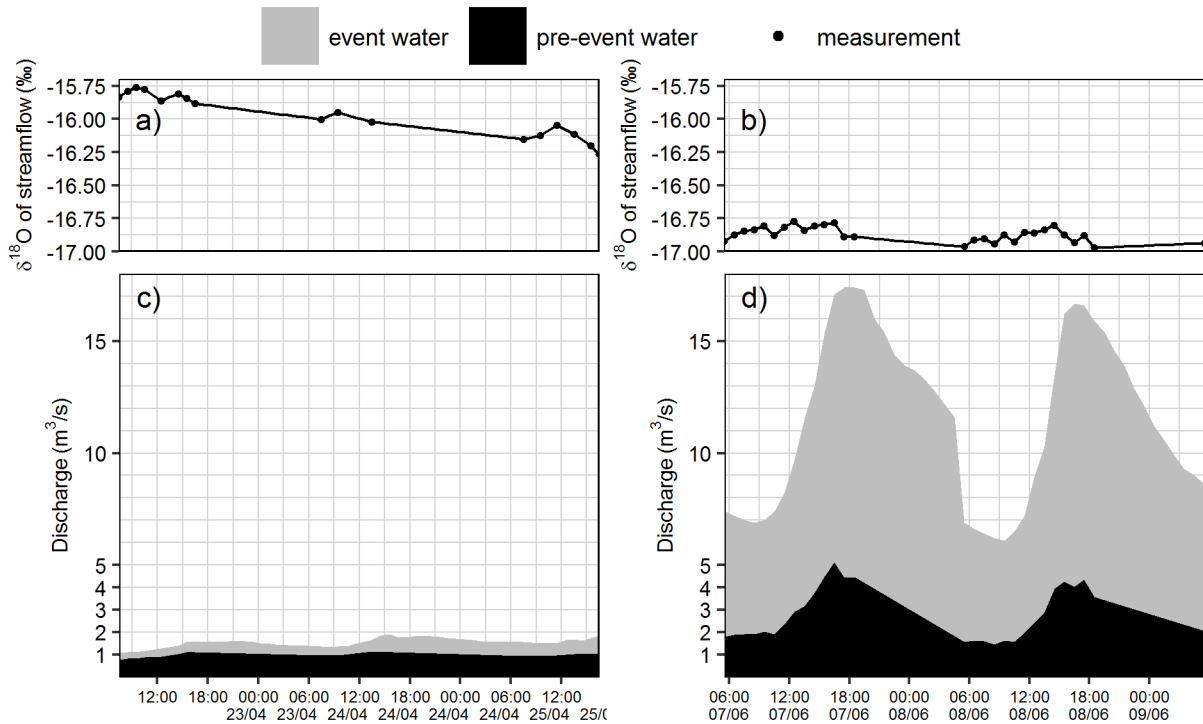


6

7  **Figure 4: Linearly interpolated stream isotopic content of Rofenache for (a) the early melt and (b) the peak melt**
8  **event. Dots indicate measurements. Event and pre-event water contributions during (c) the early melt and (d) the**
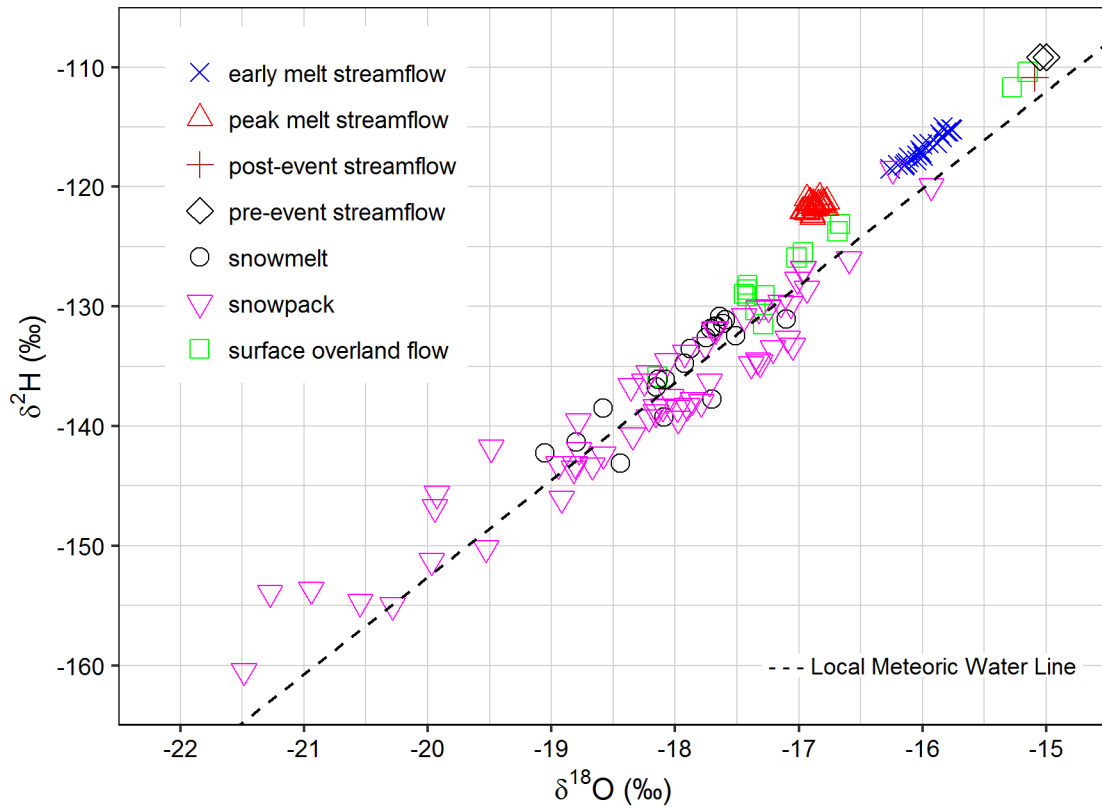9  **peak melt event calculated with the VWS approach.**

22

1

2



3

4 **Figure 5: Relationship between $\delta^2H$ and $\delta^{18}O$ values of water sources sampled during the snowmelt season 2014 in the**
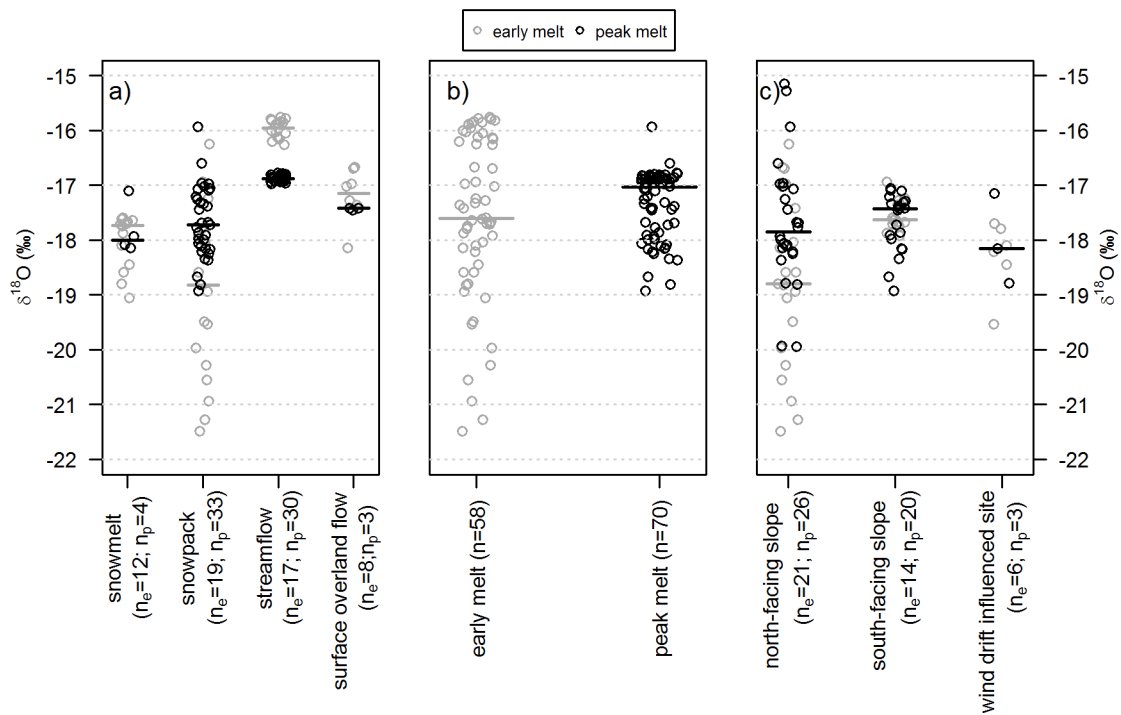5 **Rofen valley, Austrian Alps.**

6



7

8 **Figure 6: Jittered dot plots for $\delta^{18}O$ of collected water samples split into (a) water sources, (b) stage of snowmelt and**
9 **(c) spatial origin. Grey circles indicate early melt samples and black circles are for peak melt samples. The grey and**

black line represents the median of early and peak melt data, respectively. $N_e$ is the number of early melt samples and
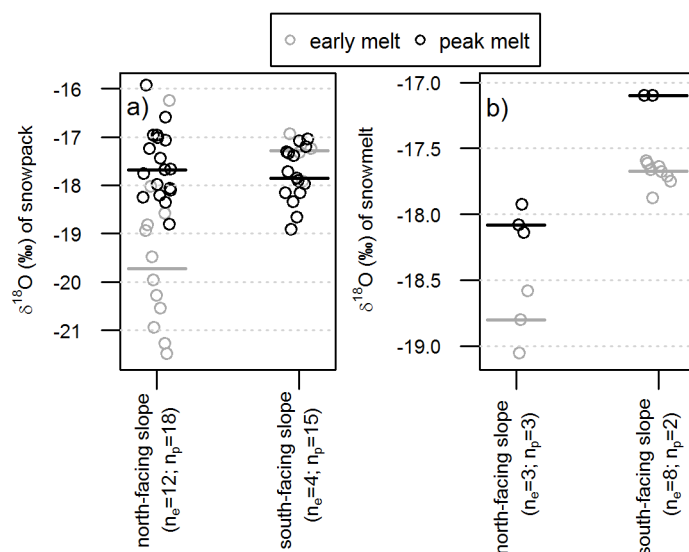
2  $n_p$ is the number of peak melt samples.



3

4   **Figure 7: Jittered dot plots for $\delta^{18}O$ of (a) snowpack and (b) snowmelt of north- and south-facing slopes. Grey circles**
5   **indicate early melt samples and black circles are for peak melt samples. The grey and black line indicates the median**
6   **of the early and peak melt data, respectively. $N_e$ is the number of early melt samples and $n_p$ is the number of peak**
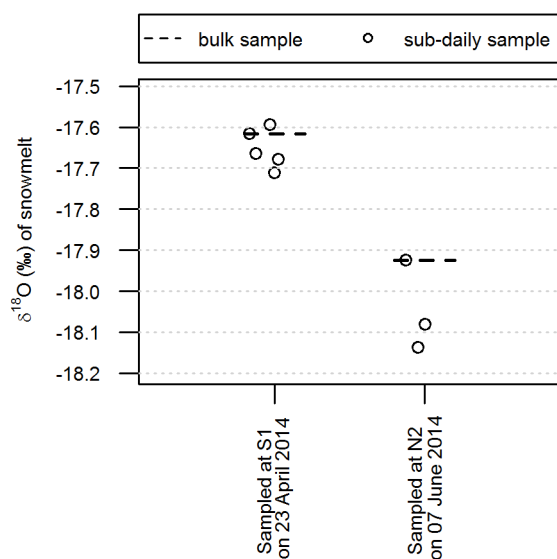7   **melt samples.**



8

9   **Figure 8: Comparison of snowmelt $\delta^{18}O$ between bulk sample (dashed line) and sub-daily samples (circles) for two**
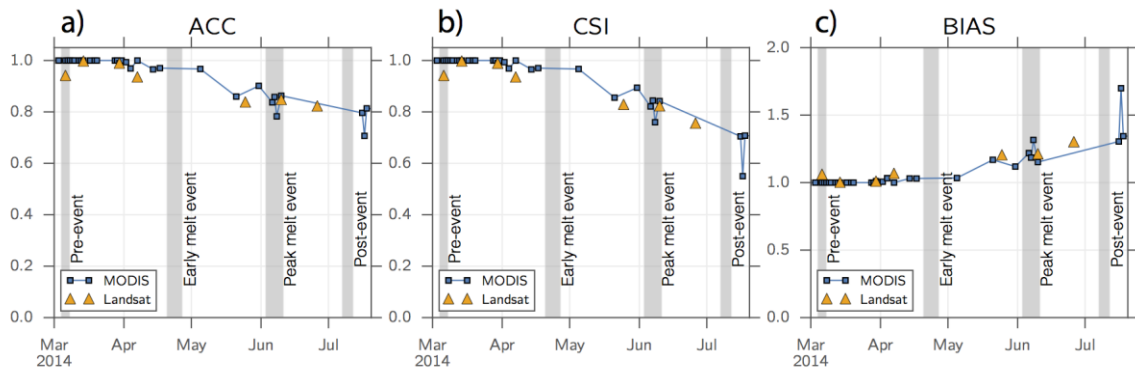10  **sites (S1, N2).**

11

12

Figure 9: Performance measures (a) Accuracy (ACC), (b) Critical Success Index (CSI), and (c) BIAS as calculated by comparing AMUNDSEN simulation results with satellite-derived (MODIS/Landsat) snow maps.
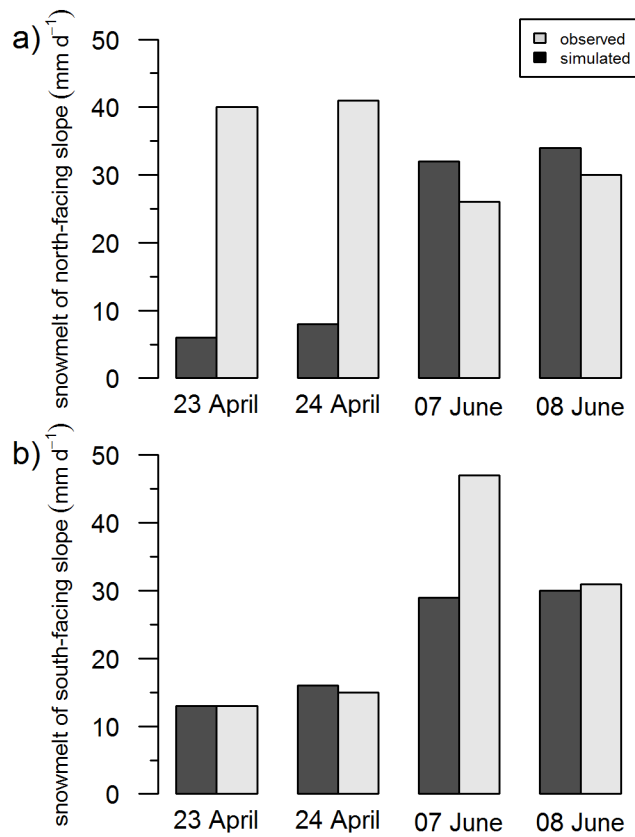


Figure 10: Differences between the observed (plot scale) and simulated (catchment scale) daily snowmelt on (a) the north-facing and (b) the south-facing slope for the early melt (23/24 April) and peak melt (07/08 June).
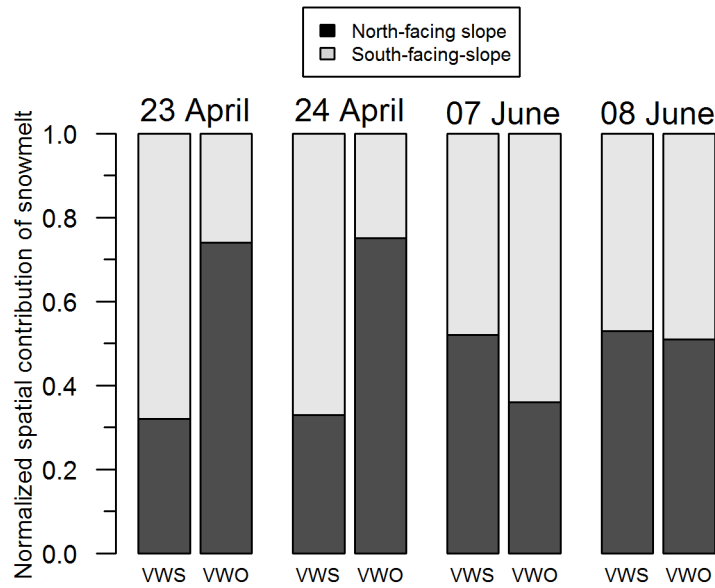
Figure 11: Comparison of the spatial contribution of weighting approaches. VWS: volume-weighted with simulated (areal) melt rates. VWO: volume-weighted with observed (plot-scale) melt rates.
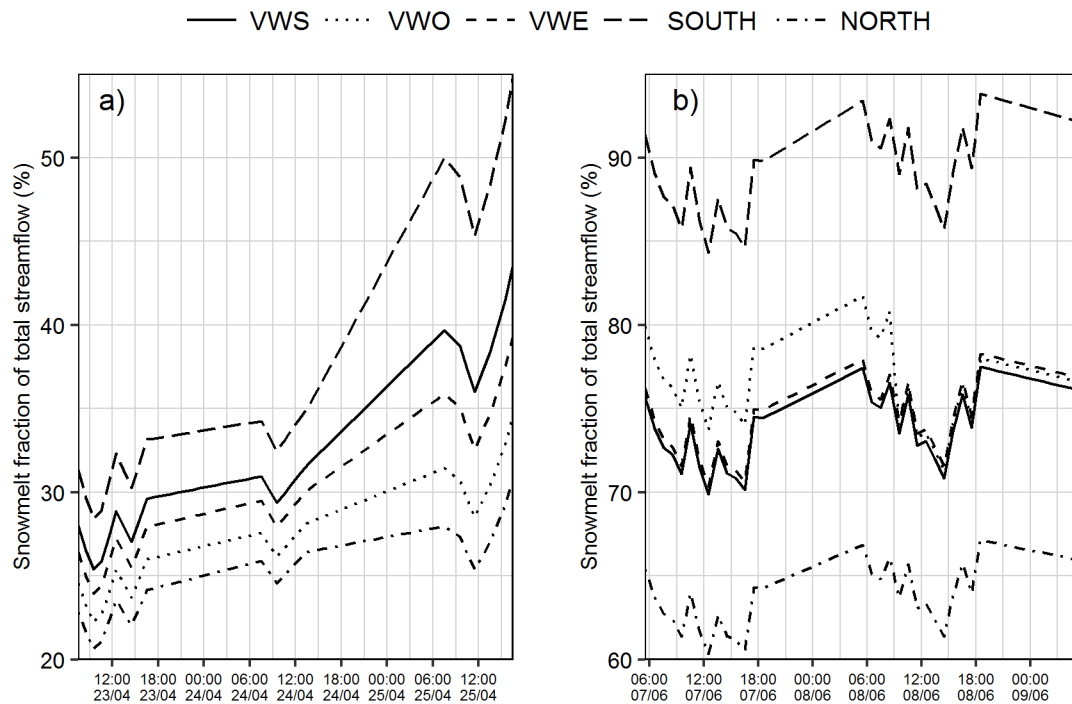


Figure 12: Comparison of weighting techniques used for estimating snowmelt fraction with IHS during (a) early melt and (b) peak melt. Scale of Y-axis in b) differs from that in a).

Table 1: Average isotopic content of snowpack and snowmelt with standard deviation for north- and south-facing slopes during the early and the peak melt event. Values are averages of three consecutive days.

| | North-facing slope | | South-facing slope | |
|---|---|---|---|---|
| | Snowpack $\delta^{18}O$ (‰) | Snowmelt $\delta^{18}O$ (‰) | Snowpack $\delta^{18}O$ (‰) | Snowmelt $\delta^{18}O$ (‰) |

| | | | | |
|---|---|---|---|---|
| **Early melt event** | -19.7±0.6 (n=12) | -18.8±0.2 (n=3) | -17.3±0.3 (n=4) | -17.4±0.2 (n=8) |
| **Peak melt event** | -17.6±0.4 (n=18) | -17.9±0.1 (n=3) | -17.9±0.1 (n=15) | -17.1±0.0 (n=2) |

**Table 2: Descriptive statistics of streamflow isotopic content (Rofenache) during events of the snowmelt season 2014. Data is sampled at the outlet of the basin.**

| | **Pre-event** | **Early melt** | **Peak melt** | **Post-event** |
|---|---|---|---|---|
| Date | 07/03 | 23/04 – 25/04 | 07/06 – 09/06 | 11/07 |
| Average ($\delta^{18}$O ‰) | -15.02 | -15.97 | -16.87 | -15.09 |
| Standard deviation ($\delta^{18}$O ‰) | 0.04 | 0.16 | 0.05 | n/a |
| Range ($\delta^{18}$O ‰) | 0.05 | 0.50 | 0.20 | n/a |
| Number of samples | 2 | 17 | 30 | 1 |

**Table 3: Comparison of observed and simulated (represented by the underlying pixel) SWE values at the plot-scale.**

| Site | Date | Stage of snowmelt season | SWE [mm] | | Difference between observed and simulated SWE [%] |
|---|---|---|---|---|---|
| | | | *Observed* | *Simulated* | |
| S1 | 2014-04-23 | Early melt | 141 | 151 | 7 |
| N1 | 2014-04-23 | Early melt | 351 | 356 | 1 |
| Wind | 2014-04-24 | Early melt | 201 | 229 | 14 |
| S1 | 2014-04-25 | Early melt | 113 | 78 | -31 |
| N1 | 2014-04-25 | Early melt | 270 | 293 | 9 |
| N2 | 2014-06-07 | Peak melt | 594 | 477 | -20 |
| N2 | 2014-06-08 | Peak melt | 568 | 435 | -23 |
| N2 | 2014-06-09 | Peak melt | 537 | 390 | -27 |
| Mean deviation between observed and simulated SWE | | | | | 13 |

**Table 4: Isotopic characterization of the event water component by the applied weighting techniques**

| | **Event water isotopic composition ($\delta^{18}$O ‰)** | | | |
|---|---|---|---|---|
| | 23/04 | 24/04 | 07/06 | 08/06 |
| VWS | -17.9 | -18.2 | -17.5 | -17.5 |
| VWO | -18.3 | -18.6 | -17.4 | -17.5 |
| VWE | -18.1 | -18.3 | -17.5 | -17.5 |

| | | | | |
|---|---|---|---|---|
| NORTH | -18.6 | -18.8 | -17.9 | -17.9 |
| SOUTH | -17.6 | -17.9 | -17.1 | -17.1 |

**Table 5: Discharge quantities of the Rofenache for the early and peak melt event at the outlet of the basin.**

| | Event | |
|---|---|---|
| | Early Melt | Peak Melt |
| Date | 23/04 – 25/04 | 07/06 – 09/06 |
| Mean discharge | $1.5\ \mathrm{m^3\,s^{-1}}$ | $11.5\ \mathrm{m^3\,s^{-1}}$ |
| Peak discharge | $1.9\ \mathrm{m^3\,s^{-1}}$ | $17.4\ \mathrm{m^3\,s^{-1}}$ |
| Volume runoff | 3.3 mm | 20.7 mm |
| Mean event water fraction | 35±3 % | 75±14 % |
| Peak event water fraction | 44±4 % | 78±15 % |

**Table 6: Event water contribution to streamflow estimated with different weighting techniques. The error indicates the variability (standard deviation) and the brackets depict the range.**

| | Event water contribution (%) | | | | |
|---|---|---|---|---|---|
| | VWS | VWO | VWE | NORTH | SOUTH |
| **Early melt event** | 35±6 (25-44) | 30±4 (22-35) | 33±5 (24-39) | 28±3 (21-31) | 40±9 (28-55) |
| **Peak melt event** | 75±2 (70-78) | 78±3 (71-82) | 76±2 (70-78) | 66±2 (60-67) | 90±3 (84-94) |